



# Physical versus phantom dark energy after DESI: thawing quintessence in a curved background

Bikash R. Dinda <sup>1,2</sup>★ and Roy Maartens <sup>1,2</sup>

<sup>1</sup>Department of Physics & Astronomy, University of the Western Cape, Cape Town 7535, South Africa

<sup>2</sup>National Institute for Theoretical & Computational Science, Cape Town 7535, South Africa

Accepted 2025 June 12. Received 2025 June 8; in original form 2025 May 2

## ABSTRACT

Recent data from Dark Energy Spectroscopic Instrument, in combination with other data, provide moderate evidence of dynamical dark energy,  $w \neq -1$ . In the  $w_0, w_a$  parametrization of  $w$ , there is a preference for a phantom crossing,  $w < -1$ , at redshift  $z \sim 0.5$ . In general relativity, the phantom equation of state is unphysical. Thus, it is important to check whether phantom crossing is present in other physically self-consistent models of dark energy that have equivalent evidence to the  $w_0, w_a$  parametrization. We find that thawing quintessence with non-zero cosmic curvature can fit the recent data as well as  $w_0, w_a$  in a flat background, based on both parametric and realistic scalar field evolutions. Although the realistic model does not allow  $w < -1$ , the parametrizations do allow it. However even if we allow  $w < -1$  the data do not enforce phantom crossing. Thus, the phantom crossing is an artefact of a parametrization that is not based on a physical model.

**Key words:** cosmological parameters – dark energy – cosmology: theory.

The Dark Energy Spectroscopic Instrument (DESI) Data Releases DR1 and DR2 (Calderon et al. 2024; Abdul-Karim et al. 2025; Adame et al. 2025; Lodha et al. 2025a, b) have delivered state-of-the-art precision on baryon acoustic oscillation (BAO) measurements. This has facilitated stringent constraints on the dark energy equation of state,  $w$  (Dinda 2024; Park, de Cruz Perez & Ratra 2024a, 2024b; Roy Choudhury & Okumura 2024; Chakraborty et al. 2025; Choudhury 2025; Colgáin et al. 2025a; Dinda & Maartens 2025; Dinda et al. 2025; Gialamas et al. 2025; Park & Ratra 2025; Wolf et al. 2025a). Using the parametrization

$$w(z) = w_0 + w_a \frac{z}{1+z}, \quad (1)$$

both DESI DR1 and DR2 BAO data favour a phantom crossing, from a phantom value  $w < -1$  at earlier times,  $z \gtrsim 0.5$ , to  $w > -1$  for  $z \lesssim 0.5$ . Phantom behaviour is unphysical in general relativity since energy conservation implies the growth of dark energy density with expansion,  $\dot{\rho}_{\text{de}} > 0$ .

It is implied by similar parametrizations which are not based on physical models of  $w$  (e.g. see fig. 4 in Lodha et al. 2025a). It is true that models of interacting dark energy in general relativity (Valiviita, Majerotto & Maartens 2008) can have an *effective*  $w_{\text{eff}} < -1$  while the intrinsic  $w$  is  $\geq -1$ . Similarly, modifications to general relativity (Clifton et al. 2012) can mimic phantom behaviour. However before abandoning simple physical models in general relativity, we need to check whether phantom behaviour is in fact required by the data.

For a physically motivated model, DESI data suggest that we consider dark energy models which behave close to a cosmological constant  $w = -1$  at early times, with an increase to  $w > -1$  at late

times (e.g. see figs 11 and 12 in Lodha et al. 2025a). Physically consistent examples are provided by the ‘thawing’ class of quintessence models (Linder 2008, 2015).

To investigate the robustness of this phantom crossing, we start by showing the DESI DR2 BAO data for  $\tilde{D}_M = D_M/r_d$  and  $\tilde{D}_H = D_H/r_d$  (where  $D_M$  and  $D_H$  are comoving and Hubble distances and  $r_d$  is the comoving sound horizon at baryon drag). We also show the best-fitting Lambda cold dark matter ( $\Lambda$ CDM) in the flat (Fig. 1) and negatively curved  $\text{o}\Lambda$ CDM (Fig. 2) cases, using also the CMB distance prior, as in DESI DR2 (Abdul-Karim et al. 2025) (see their appendix A). From Figs 1 and 2, it is clear that at earlier times ( $z \gtrsim 1.5$ ) the deviations from both  $\Lambda$ CDM and  $\text{o}\Lambda$ CDM model are well within  $1\sigma$ . At intermediate times ( $0.9 \gtrsim z \gtrsim 1.5$ ) the deviations are  $\sim 1\sigma$ , and at late times  $z \lesssim 0.9$  the deviations are  $\lesssim 2\sigma$ . Note that these results are similar to the lower panels of fig. 6 in Abdul-Karim et al. (2025). These plots hint that there is no evidence for deviation from  $\Lambda$ CDM (or  $\text{o}\Lambda$ CDM) at higher redshifts ( $z \gtrsim 1.5$ ). At intermediate redshifts ( $0.9 \gtrsim z \gtrsim 1.5$ ) there is no significant deviation either. This is evidence that the phantom crossing is a model-dependent artefact of the  $w_0 w_a$  CDM model. Evidently, the  $w_0 w_a$  CDM or similar parametrizations are too simplistic to correctly capture the behaviour at lower and higher redshifts simultaneously and they may worsen the  $H_0$  tension (Colgáin et al. 2025a). Here, we focus on the implications of DESI data for dynamical dark energy, without considering the possible problems introduced by systematics (see e.g. Sapone & Nesseris 2024; Colgáin & Sheikh-Jabbari 2025; Colgáin et al. 2025a; Colgáin, Pourjaghi & Sheikh-Jabbari 2025b).

Figs 1 and 2 also reveal another interesting feature. In flat  $\Lambda$ CDM,  $\tilde{D}_H = \tilde{D}'_M$  so that the deviations in  $\tilde{D}_M$  and  $\tilde{D}_H$  should be similar in the flat case. However, DESI DR2 data shows that the deviations are different in  $\tilde{D}_M$  and  $\tilde{D}_H$  at intermediate redshifts. The DESI DR2

\* E-mail: [bikashrdinda@gmail.com](mailto:bikashrdinda@gmail.com)

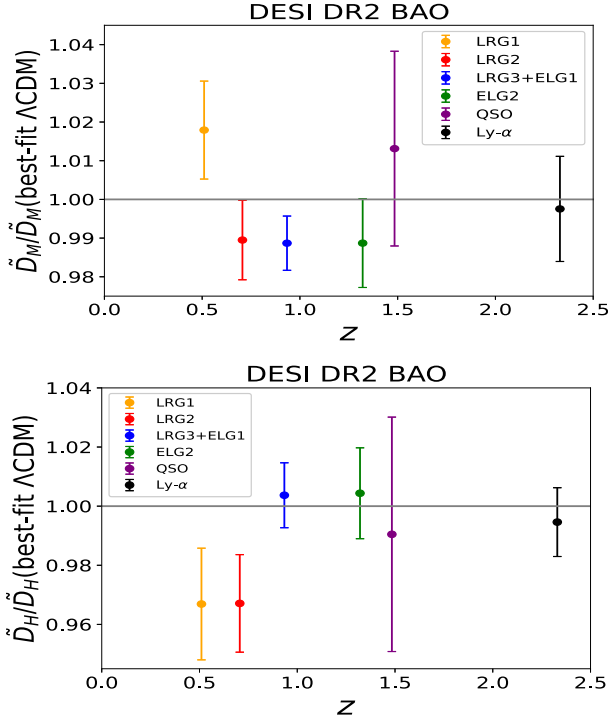


**Figure 1.** Comparison of  $\tilde{D}_M = D_M/r_d$  (upper panel) and  $\tilde{D}_H = D_H/r_d$  (lower panel) to the best-fitting values of flat  $\Lambda$ CDM, obtained from CMB+DESI DR2 BAO.

main paper (Abdul-Karim et al. 2025) finds the constraint  $10^3\Omega_{K0} = 2.3 \pm 1.1$  on cosmic curvature (their table V). Of course, inferences about curvature may not hold for dynamical dark energy, since in that case,  $w$  is partially degenerate with  $\Omega_{K0}$ . Cosmic curvature directly affects distances by altering the geometry of photon paths (Liu et al. 2020; Wei & Melia 2020; Dinda 2025). Because it evolves as  $(1+z)^2$ , curvature has its strongest relative effect in the narrow redshift window between matter domination and dark energy domination, when its influence is seen only through its contribution to the energy budget.

At this stage, our task is half complete, because the intermediate to higher redshift behaviour can be well modelled by the  $\text{o}\Lambda$ CDM model, but definitely not the lower redshift results. The lower redshift data is what allows  $w_0w_a$ CDM or similar parametrizations to show a hint of deviations from  $\Lambda$ CDM and of phantom crossing even in the presence of non-zero cosmic curvature. The  $\text{o}\Lambda$ CDM model cannot properly capture the behaviour over the entire redshift range either. Consequently, our next step is to find a physically consistent model which can capture the behaviour for the whole redshift range.

We consider quintessence dark energy models, which have self-consistent physical properties, including  $w \geq -1$  and a speed of sound  $c_s = 1$  (Caldwell, Dave & Steinhart 1998; Caldwell & Linder 2005; Tsujikawa 2013). Quintessence models cover a huge range of behaviour, but we focus on the thawing class (TQ) which naturally produces  $w > -1$  at low redshift, as suggested by the predictions in  $w_0w_a$ CDM and similar parametrizations; see fig. 4 in Lodha et al. (2025a). We also include cosmic curvature ( $\text{oTQ}$ ). For generality, we use two parametrizations of  $w$  which approximate thawing quintessence models (Carvalho et al. 2006; Linder 2008, 2015; Abreu & Turner 2025; Akthar & Hossain 2025; Shlivko, Steinhart & Steinhart 2025)

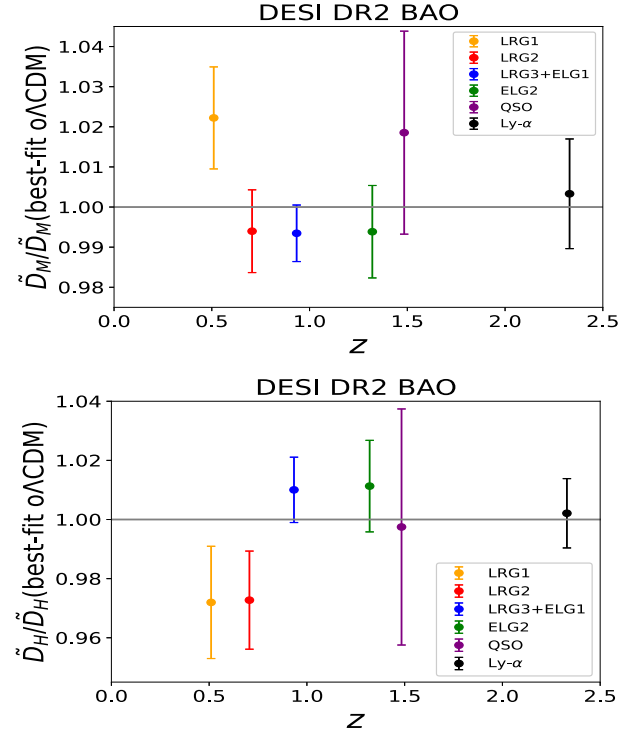


**Figure 2.** As in Fig. 1 but for best-fitting  $\text{o}\Lambda$ CDM values.

$$w(z) = -1 + \frac{1 + w_0}{(1+z)^3}, \quad (2)$$

$$w(z) = -1 + \frac{3^{2/3}(1+w_0)(z^3 + 3z^2 + 3z + 3)^{-2/3}}{1+z}. \quad (3)$$

We identify these 1-parameter  $w$  models as  $\text{oTQ1}$  and  $\text{oTQ2}$ . The Hubble rate is given by

$$\frac{H^2}{H_0^2} = \Omega_{r0}(1+z)^4 + \Omega_{m0}(1+z)^3 + \Omega_{K0}(1+z)^2 + \Omega_{q0} \exp \left[ 3 \int_0^z \frac{1+w(\tilde{z})}{1+\tilde{z}} d\tilde{z} \right], \quad (4)$$

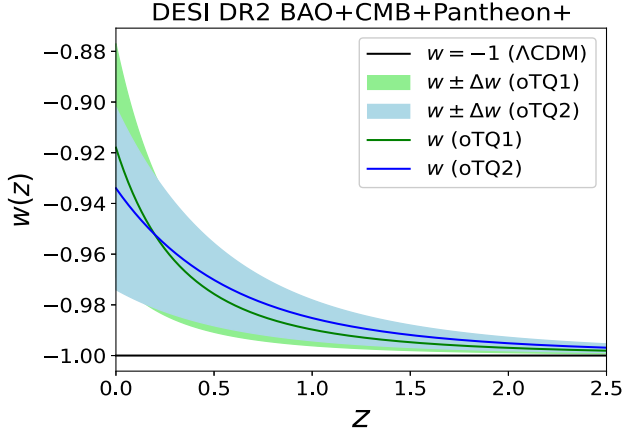
where  $\Omega_{r0} + \Omega_{m0} + \Omega_{K0} + \Omega_{q0} = 1$ .

Fig. 3 shows the mean  $w(z)$  for  $\text{oTQ1,2}$  as given by equations (2) and (3), with  $1\sigma$  shaded regions. Constraints are from DESI DR2 BAO+CMB+Pantheon+. The full (realistic) quintessence models (described later), with  $w \equiv w_\phi = p_\phi/\rho_\phi$ , do not allow  $w < -1$ , but this is not automatically enforced in the  $w(z)$  parametrizations  $\text{oTQ1,2}$  above. However, even if we impose a prior  $w_0 < -1$  in the data analysis, it does not alter the results in Fig. 3. This shows that there is no evidence of phantom crossing in these models.

In order to make a stronger statement, we should show that the  $\text{oTQ}$  models are at the same (or better) evidence level as  $w_0w_a$ CDM. To this end, we compare the best-fitting log-likelihood values of these models

$$\ln L(\text{oTQ1, 2}) - \ln L(w_0w_a\text{CDM}) = (0.47, 0.37). \quad (5)$$

Since the number of parameters is the same in all three models ( $w_0, \Omega_{K0}$  in  $\text{oTQ1,2}$ ), the best-fitting log-likelihood comparison is enough to show the model comparison. We see that  $\text{oTQ1}$  and  $\text{oTQ2}$  are slightly preferred over  $w_0w_a$ CDM. Although this is not significant, it is enough to show that the phantom crossing is not inevitable or even preferred.



**Figure 3.** Thawing quintessence models oTQ1,2. Constraints on  $w_0$  are from DESI DR2 BAO+CMB+Pantheon+.

Note that in general, models of quintessence worsen the  $H_0$  tension (Vagnozzi 2020; Banerjee et al. 2021; Di Valentino et al. 2021; Dinda 2022; Lee et al. 2022), but we checked the constraints on  $H_0$  and found no significant differences between these three models. Thus, this tension is not improved or worsened by the thawing quintessence models with non-zero cosmic curvature.

A dark energy parametrization is a simple and useful way to do data analysis in cosmology – but preferably we need to show that a physically motivated model of dark energy, in this case a realistic thawing quintessence, produces similar results (Velten, vom Marttens & Zimdahl 2014; Goldstein et al. 2023; Ramadan, Sakstein & Rubin 2024; Tada & Terada 2024; Wolf et al. 2024; Akrami, Alestas & Nesseris 2025; Berbig 2025; Borghetto et al. 2025; Dubey et al. 2025; Lodha et al. 2025b; Payeur, McDonough & Brandenberger 2025; Shajib & Frieman 2025; Steinhardt, Phillips & Wojtak 2025; Wolf, García-García & Ferreira 2025b). We consider a class of realistic thawing quintessence models in the presence of cosmic curvature. In the presence of matter, radiation, and curvature, a general quintessence field obeys the evolution equations (Clemson & Liddle 2009; Dinda 2017; Andriot et al. 2024; Bhattacharya et al. 2024)

$$\begin{aligned}
 \frac{dw}{dN} &= (w - 1) \left( 3w + 3 - \lambda \sqrt{3(w + 1)\Omega_q} \right), \\
 \frac{d\Omega_q}{dN} &= \Omega_q [3w\Omega_q - 3w - \Omega_K + \Omega_r], \\
 \frac{d\lambda}{dN} &= -\sqrt{3}(\Gamma - 1)\lambda^2 \sqrt{(w + 1)\Omega_q}, \\
 \frac{d\Omega_r}{dN} &= \Omega_r [3w\Omega_q - \Omega_K + \Omega_r - 1], \\
 \frac{d\Omega_K}{dN} &= \Omega_K [3w\Omega_q - \Omega_K + \Omega_r + 1],
 \end{aligned} \tag{6}$$

where  $N = \ln a$ , the slope of the quintessence potential is  $\lambda = -M_{\text{pl}} \partial_\phi V / V$  and  $\Gamma = V \partial_\phi^2 V / (\partial_\phi V)^2$ . For non-constant  $\Gamma$  and which cannot be explicitly expressed in terms of  $\lambda$ , one needs further differential equations that depend on the nature of the potential. We restrict our analysis to constant  $\Gamma$ , which includes exponential ( $\Gamma = 1$ ) and monomial ( $\Gamma = 1 + 1/n$  for  $V(\phi) = V_0 \phi^{-n}$ ) potentials.

For thawing quintessence, initial values should be  $0 < w_i + 1 \ll 1$  and  $\lambda_i > 0$  (Scherrer & Sen 2008; Clemson & Liddle 2009; Chiba, De Felice & Tsujikawa 2013; Tsujikawa 2013; Dinda & Sen 2018).

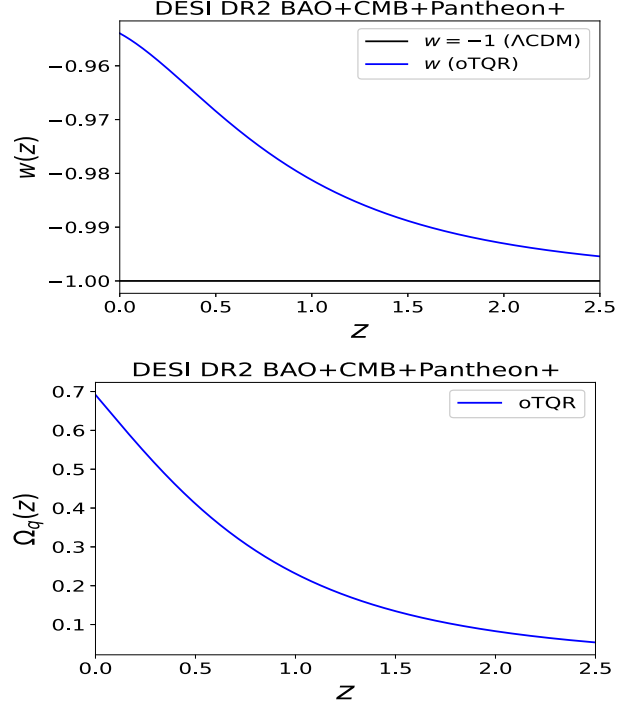


**Figure 4.**  $w(z)$  (upper panel) and  $\Omega_q(z)$  (lower panel) for a realistic thawing quintessence model (oTQR) with best-fitting values obtained from DESI DR2 BAO+CMB+Pantheon+.

We use  $w_i = 10^{-4} - 1$  and  $\Gamma = 5$  ( $n = 1/4$ ). We name this model oTQR (curved thawing quintessence realistic).

Using the best-fitting cosmological density parameters from DESI DR2 BAO+CMB+Pantheon+ data, we can solve the system in equation (6). The resulting  $w(z)$  and  $\Omega_q(z)$  are shown in Fig. 4. Fig. 5 shows constraints on the model parameters through triangle plots.

In order to find proper constraints on realistic quintessence parameters, we need to have data-informed priors on these parameters (Lodha et al. 2025a). However, this is true only for the energy density parameters  $\Omega_{q_i}$ ,  $\Omega_{r_i}$ , and  $\Omega_{K_i}$ , not for the other parameters. This is due to the cosmic coincidence problem, present in all realistic physical models (Zlatev, Wang & Steinhardt 1999; Sahni & Starobinsky 2000; Velten et al. 2014). If we try to mimic  $w_0 w_a$ CDM by a physically motivated model, we will encounter the same coincidence problem. Thus, this fact cannot be a negative point for model comparison.

It is also argued in Lodha et al. (2025a) that for realistic quintessence models to fit the data well, they must have a rapid increase of  $w$  for  $z \lesssim 0.3$ . However, the upper panel of Fig. 4 shows that this statement is not applicable. Furthermore, it is argued that there might be features of a sharp increase in the energy density of dark energy – but the lower panel of Fig. 4 shows no sharp increase.

Finally, we compare the best-fitting log-likelihood of the realistic open thawing quintessence model oTQR to that of  $w_0 w_a$ CDM,

$$\ln L(\text{oTQR}) - \ln L(w_0 w_a \text{CDM}) = -0.03. \tag{7}$$

This shows that the evidence for curved realistic quintessence is effectively equivalent to that of flat  $w_0 w_a$ CDM. We conclude that curved thawing quintessence is equivalently favoured compared to  $w_0 w_a$ CDM in light of DESI DR2 BAO data (in combination with other relevant observations). The evidence for phantom crossing is model dependent.

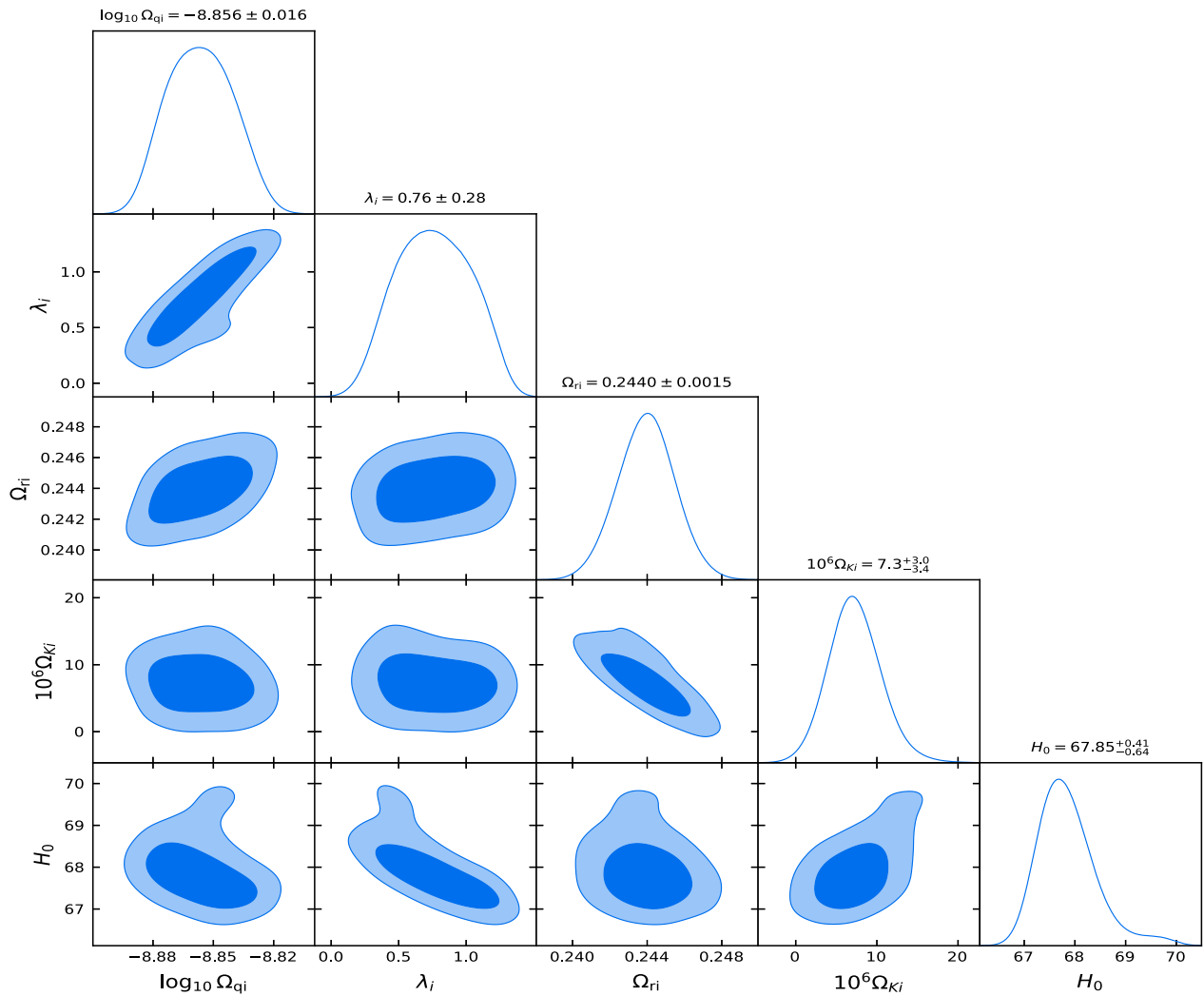


**Figure 5.** Constraints on the oTQR model parameters for DESI DR2 BAO+CMB+Pantheon+data.

## ACKNOWLEDGEMENTS

We are supported by the South African Radio Astronomy Observatory and the National Research Foundation (grant no. 75415).

## DATA AVAILABILITY

This study did not generate new data. All analysed data are publicly available and have been properly cited.

## REFERENCES

- Abdul-Karim M. et al., 2025, preprint (arXiv:2503.14738)  
 Abreu M. L., Turner M. S., 2025, preprint (arXiv:2502.08876)  
 Adame A. G. et al., 2025, *J. Cosmol. Astropart. Phys.*, 2025, 021  
 Akrami Y., Alestas G., Nesseris S., 2025, preprint (arXiv:2504.04226)  
 Akthar S., Hossain M. W., 2025, *J. Cosmol. Astropart. Phys.*, 2025, 024  
 Andriot D., Parameswaran S., Tsimpis D., Wrase T., Zavala I., 2024, *J. High Energy Phys.*, 2024, 117  
 Banerjee A., Cai H., Heisenberg L., Colgáin E. O., Sheikh-Jabbari M. M., Yang T., 2021, *Phys. Rev. D*, 103, L081305  
 Berbig M., 2025, *J. Cosmol. Astropart. Phys.*, 2025, 015  
 Bhattacharya S., Borghetto G., Malhotra A., Parameswaran S., Tasinato G., Zavala I., 2024, *J. Cosmol. Astropart. Phys.*, 2024, 073  
 Borghetto G., Malhotra A., Tasinato G., Zavala I., 2025, preprint (arXiv:2503.11628)  
 Calderon R. et al., 2024, *J. Cosmol. Astropart. Phys.*, 2024, 048  
 Caldwell R. R., Linder E. V., 2005, *Phys. Rev. Lett.*, 95, 141301  
 Caldwell R. R., Dave R., Steinhardt P. J., 1998, *Phys. Rev. Lett.*, 80, 1582  
 Carvalho F. C., Alcaniz J. S., Lima J. A. S., Silva R., 2006, *Phys. Rev. Lett.*, 97, 081301  
 Chakraborty A., Chanda P. K., Das S., Dutta K., 2025, preprint (arXiv:2503.10806)  
 Chiba T., De Felice A., Tsujikawa S., 2013, *Phys. Rev. D*, 87, 083505  
 Choudhury S. R., 2025, preprint (arXiv:2504.15340)  
 Clemson T. G., Liddle A. R., 2009, *MNRAS*, 395, 1585  
 Clifton T., Ferreira P. G., Padilla A., Skordis C., 2012, *Phys. Rept.*, 513, 1  
 Colgáin E. O., Sheikh-Jabbari M. M., 2025, preprint (arXiv:2412.12905)  
 Colgáin E. O., Pourojaghi S., Sheikh-Jabbari M. M., Yin L., 2025a, preprint (arXiv:2504.04417)  
 Colgáin E. O., Pourojaghi S., Sheikh-Jabbari M. M., 2025b, preprint (arXiv:2505.19029)  
 Di Valentino E. et al., 2021, *Class. Quantum Gravity*, 38, 153001  
 Dinda B. R., 2017, *J. Cosmol. Astropart. Phys.*, 2017, 035  
 Dinda B. R., 2022, *Phys. Rev. D*, 105, 063524  
 Dinda B. R., 2024, *J. Cosmol. Astropart. Phys.*, 2024, 062  
 Dinda B. R., 2025, *Phys. Rev. D*, 111, 103533  
 Dinda B. R., Maartens R., 2025, *J. Cosmol. Astropart. Phys.*, 2025, 120  
 Dinda B. R., Sen A. A., 2018, *Phys. Rev. D*, 97, 083506

- Dinda B. R., Maartens R., Saito S., Clarkson C., 2025, preprint (arXiv:2504.09681)
- Dubey S., Agrawal S., Beesham A., Sofuoğlu D., Shukla B. K., 2025, *Eur. Phys. J. Plus*, 140, 254
- Gialamas I. D., Hütsi G., Kannike K., Racioppi A., Raidal M., Vasar M., Veermäe H., 2025, *Phys. Rev. D*, 111, 043540
- Goldstein S., Park M., Raveri M., Jain B., Samushia L., 2023, *Phys. Rev. D*, 107, 063530
- Lee B.-H., Lee W., Colgáin E. O., Sheikh-Jabbari M. M., Thakur S., 2022, *J. Cosmol. Astropart. Phys.*, 2022, 004
- Linder E. V., 2008, *Gen. Relativ. Gravit.*, 40, 329
- Linder E. V., 2015, *Phys. Rev. D*, 91, 063006
- Liu Y., Cao S., Liu T., Li X., Geng S., Lian Y., Guo W., 2020, *ApJ*, 901, 129
- Lodha K. et al., 2025a, preprint (arXiv:2503.14743)
- Lodha K. et al., 2025b, *Phys. Rev. D*, 111, 023532
- Park C.-G., Ratra B., 2025, preprint (arXiv:2501.03480)
- Park C.-G., de Cruz Perez J., Ratra B., 2024a, preprint (arXiv:2410.13627)
- Park C.-G., de Cruz Pérez J., Ratra B., 2024b, *Phys. Rev. D*, 110, 123533
- Payeur G., McDonough E., Brandenberger R., 2025, preprint (arXiv:2411.13637)
- Ramadan O. F., Sakstein J., Rubin D., 2024, *Phys. Rev. D*, 110, L041303
- Roy Choudhury S., Okumura T., 2024, *ApJ*, 976, L11
- Sahni V., Starobinsky A. A., 2000, *Int. J. Mod. Phys. D*, 09, 373
- Sapone D., Nesseris S., 2024, preprint (arXiv:2412.01740)
- Scherrer R. J., Sen A. A., 2008, *Phys. Rev. D*, 77, 083515
- Shajib A. J., Frieman J. A., 2025, preprint (arXiv:2502.06929)
- Shlivko D., Steinhardt P. J., Steinhardt C. L., 2025, preprint (arXiv:2504.02028)
- Steinhardt C. L., Phillips P., Wojtak R., 2025, preprint (arXiv:2504.03829)
- Tada Y., Terada T., 2024, *Phys. Rev. D*, 109, L121305
- Tsujikawa S., 2013, *Class. Quantum Gravity*, 30, 214003
- Vagnozzi S., 2020, *Phys. Rev. D*, 102, 023518
- Valiviita J., Majerotto E., Maartens R., 2008, *J. Cosmol. Astropart. Phys.*, 2008, 020
- Velten H. E. S., vom Martens R. F., Zimdahl W., 2014, *Eur. Phys. J. C*, 74, 3160
- Wei J.-J., Melia F., 2020, *ApJ*, 888, 99
- Wolf W. J., García-García C., Bartlett D. J., Ferreira P. G., 2024, *Phys. Rev. D*, 110, 083528
- Wolf W. J., García-García C., Anton T., Ferreira P. G., 2025a, preprint (arXiv:2504.07679)
- Wolf W. J., García-García C., Ferreira P. G., 2025b, *J. Cosmol. Astropart. Phys.*, 2025, 034
- Zlatev I., Wang L.-M., Steinhardt P. J., 1999, *Phys. Rev. Lett.*, 82, 896

This paper has been typeset from a  $\text{\TeX/L\AA\TeX}$  file prepared by the author.